

# An operational procedure for rapid flood risk assessment in Europe

**Francesco Dottori, Milan Kalas, Peter Salamon, Alessandra Bianchi, Lorenzo Alfieri, Luc Feyen**

European Commission, Joint Research Centre, Directorate for Space, Security and Migration, Via E. Fermi 2749, 21027 Ispra, Italy.

francesco.dottori@ec.europa.eu

**Keywords:** real-time, early warning system, flood hazard mapping, flood impact, economic damage, population, risk assessment

## *Abstract*

The development of methods for rapid flood mapping and risk assessment is a key step to increase the usefulness of flood early warning systems, and is crucial for effective emergency response and flood impact mitigation. Currently, flood early warning systems rarely include real-time components to assess potential impacts generated by forecast flood events. To overcome this limitation, this work describes the benchmarking of an operational procedure for rapid flood risk assessment based on predictions issued by the European Flood Awareness System (EFAS). Daily streamflow forecasts produced for major European river networks are translated into event-based flood hazard maps using a large map catalogue derived from high-resolution hydrodynamic simulations. Flood hazard maps are then combined with exposure and vulnerability information, and the impacts of the forecast flood events are evaluated in terms of flood prone areas, economic damage and affected population, infrastructures and cities.

An extensive testing of the operational procedure is carried out by analysing the catastrophic floods of May 2014 in Bosnia-Herzegovina, Croatia and Serbia. The reliability of the flood mapping methodology is tested against satellite-based and report-based flood extent data, while modelled estimates of economic damage and affected population are compared against ground-based estimations. Finally, we evaluate the skill of risk estimates derived from EFAS flood forecasts with different lead times and combinations of probabilistic forecasts. Results show the potential of the real-time operational procedure in helping emergency response and management.

## *1) Introduction*

Nowadays, flood early warning systems (EWS) have become key components of flood management strategies in many rivers (Cloke et al., 2013; Alfieri et al., 2014a). They can increase

37 preparedness of authorities and population, thus helping reduce negative impacts (Pappenberger  
38 et al., 2015). Early warning is particularly important for cross-border river basins where  
39 cooperation between authorities of different countries may require more time to inform and  
40 coordinate actions (Thielen et al., 2009).

41 In this context, the European Commission has developed the European Flood Awareness System  
42 (EFAS) which provides operational flood predictions in major European rivers as part of the  
43 Copernicus Emergency Management Services. The service is fully operational since 2012 and  
44 available to hydro-meteorological services with responsibility in flood warning, EU civil  
45 protection and their network.

46 While early warning systems are routinely used to predict flood magnitude, there is still a gap in  
47 the ability to translate flood forecasts into risk forecasts, that is, to evaluate the possible  
48 consequences generated by forecast events (e.g. flood prone areas, affected population, flood  
49 damages losses), given their probability of occurrence. Generally, flood impacts are evaluated  
50 considering reference risk scenarios where a fixed return period is used for all the area of interest,  
51 for instance based on official maps issued by competent authorities (EC 2007). However, this  
52 implies some degree of interpretation to define flood impact and risk in case of a flood forecast.  
53 A few research projects are being developed where flood impact estimation is automated and  
54 linked to event forecasting (Rossi et al., 2015; Schulz et al., 2015; Saint-Martin et al., 2016),  
55 however to our knowledge these systems are still at experimental phase, and not yet integrated  
56 into operational EWS.

57 The availability of real-time operational systems for assessing potential consequences of forecast  
58 events would be a substantial advance in helping emergency response (Molinari et al., 2013), and  
59 indeed flood risk forecasts are increasingly being requested by end users of early warning systems  
60 (Emerton et al., 2016; Ward et al., 2015). At local scale, the joint evaluation of flood probabilities  
61 and consequences may not only increase preparedness of emergency services, but also allow cost-  
62 benefit considerations for planning and prioritizing response measures (e.g. strengthening flood  
63 defences, planning evacuation of people at risk). At European scale, the possibility to receive  
64 prior information on expected flood risk would help the Emergency Response Coordination  
65 Centre (ERCC) in prioritizing and coordinating support to national emergency services.

66 In the present paper, we describe a methodology designed to meet the needs of EWS users and  
67 overcome the limitations mentioned so far. The methodology translates EFAS flood forecasts into  
68 event-based flood hazard maps, and combines hazard, exposure and vulnerability information to  
69 produce risk estimations in near-real time. All the components are fully integrated within the  
70 EFAS forecasting system, thus providing seamless risk forecasts at European scale.

71 To demonstrate the reliability of the proposed methodology, we perform a detailed assessment  
72 focused on the 2014 floods in the Sava River Basin in Southeast Europe. A large dataset for the  
73 evaluation of the results has been collected, which consists of observed flood magnitude, flood  
74 extent derived from different satellite imagery datasets, and detailed post-event evaluation of  
75 flood impacts, economic damage assessment and affected population and infrastructure.

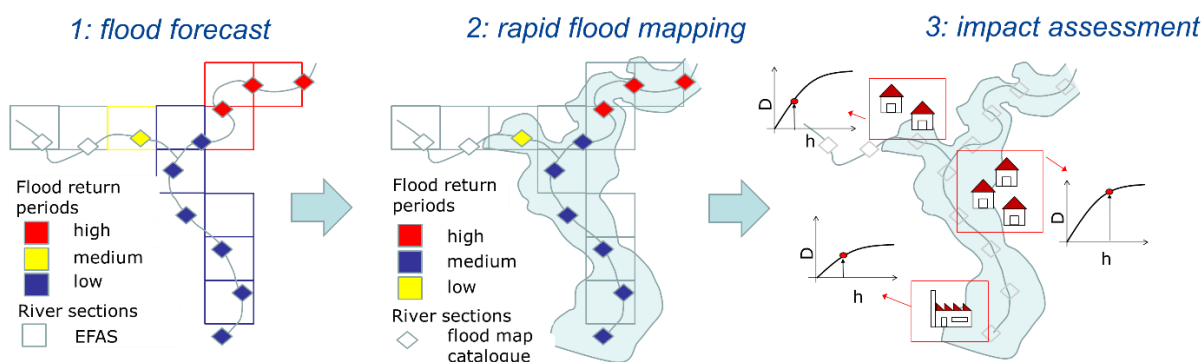
76 The reliability of the flood mapping procedure is first assessed by assuming a “perfect” forecast,  
 77 where flood magnitude is taken from real observations instead of EFAS predictions. The effect  
 78 of flood defences failure is also taken into account. After that, we test the performance of the  
 79 operational flood forecasting procedure, to evaluate the influence of different lead times and  
 80 combination of forecast members.

## 81 2) Methodology

82

83 In this section we describe the three components which compose the rapid risk assessment  
 84 procedure: 1) streamflow and flood forecasting; 2) event-based rapid flood hazard mapping 3)  
 85 impact assessment. Figure 1 shows a conceptual scheme of the steps composing the methodology.

86



87

88 *Figure 1: conceptual scheme of the rapid risk assessment procedure*

89

90 The basic workflow of the procedure is the following:

- 91 • Every time a new forecast is available, we evaluate the river sections potentially affected and  
 92 local flood magnitude, expressed as return period of the peak discharge;
- 93 • we identify areas at risk of flooding using a map catalogue, which defines all the flood prone  
 94 areas for each river section and flood magnitude; these local flood maps are then compared  
 95 against local flood protection levels and merged to derive event-based hazard maps;
- 96 • Event hazard maps are combined with exposure and vulnerability information to assess  
 97 affected population, infrastructures and urban areas, and economic damage.

98

99 The described procedure is fully integrated in the existing EFAS forecast analysis chain and run  
 100 in near-real time. When a new EFAS hydrological forecast becomes available (step 1), the risk  
 101 assessment procedure is activated in those locations where predicted peak discharges exceeds the  
 102 flood protection levels (step 2). When activated, the execution time depends on the extent and  
 103 spatial spread of the affected areas over the full forecasting domain. Even in case of flood events  
 104 occurring simultaneously in different European countries, the results of the analysis are delivered  
 105 within one hour after the EFAS forecast runs are finished.

106 The following sections provide a detailed description of each component.

## 107 *2.1 Flood forecast: the European Flood Awareness System (EFAS)*

108

109 The European Flood Awareness System (EFAS) produces streamflow forecasts for Europe using  
110 a hydrological model driven by daily weather forecasts. We provide here a general description of  
111 the EFAS components, the reader is referred to the website ([www.efas.eu](http://www.efas.eu)) and to published  
112 literature for further details (Thielen et al., 2009; Pappenberger et al., 2011; Cloke et al., 2013;  
113 Alfieri et al., 2014a).

114 Hydrological simulations in EFAS are performed with Lisflood (Burek et al, 2013; van der Knijff  
115 et al., 2010), a distributed physically based rainfall-runoff model combined with a routing module  
116 for river channels. The model is calibrated at European scale using streamflow data from a large  
117 number of river gauges and meteorological fields interpolated from point measurements of  
118 precipitation and temperature. Based on this calibration, a reference hydrological simulation for  
119 the period 1990-2013 is run for the European window at 5 km grid spacing, and updated daily.  
120 This reference simulation provides initial conditions for daily forecast runs of the Lisflood model  
121 driven by the latest weather predictions, which are provided twice per day with lead times up to  
122 10 days. The reference simulation is also used to estimate discharge values for the return periods  
123 corresponding to 1, 2, 5 and 20-year at every point of the river network. All flood forecasts are  
124 compared against these discharge thresholds and the threshold exceedance is calculated. In case  
125 the 5 year threshold is consistently exceeded over 3 consecutive forecasts, flood warnings for the  
126 affected locations are issued to the members of the EFAS consortium. The persistence criterion  
127 has been introduced to reduce the number of false alarms and focus on large fluvial floods caused  
128 mainly by widespread severe precipitation, combined rainfall with snow-melting or prolonged  
129 rainfalls of medium intensity.

130 To account for the inherent uncertainty of the weather forecast, EFAS adopts a multi-model  
131 ensemble approach, running the hydrological model with forecasts provided by the European  
132 Centre for Medium Weather Forecast (ECMWF), the Consortium for Small-scale Modelling  
133 (COSMO), and the Deutscher Wetterdienst (DWD).

## 134 *2.2 Rapid flood hazard mapping*

### 135 *2.2.1 Database of flood hazard maps*

136

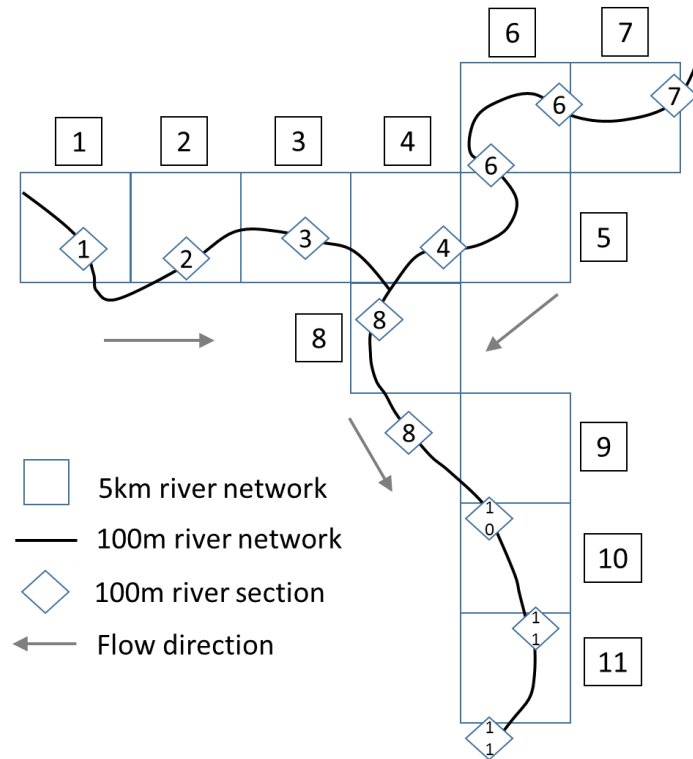
137 Linking streamflow forecast with inundation mapping is complex because inundation modelling  
138 tools are computationally much more demanding than hydrological models used in early warning  
139 systems, which currently prevent a real time integration of these two components. To overcome  
140 this limitation, in the present work we decided to create a catalogue of flood inundation maps  
141 covering all the EFAS river network and linked to EFAS streamflow forecast.

142 The hydrological input for creating the map catalogue is derived from the streamflow dataset of  
143 the EFAS reference simulation, described in Section 2.1. The information is available on the  
144 EFAS river network at 5km grid spacing for rivers with upstream drainage areas larger than 500

145 km<sup>2</sup>. Since hydrographs simulated in the EFAS reference simulation are not referred to specific  
146 return periods, we use a statistical analysis of extreme values to derive peak discharges in every  
147 cell of the river network for reference return periods of 10, 20, 50, 100, 200 and 500 years. In  
148 addition, we extract flow duration curves from the reference simulation which are used together  
149 with peak discharges to calculate synthetic flood hydrographs (see Alfieri et al., 2014b for a  
150 detailed description).

151 The streamflow data is then downscaled to a high-resolution river network (100m), where  
152 reference sections are identified at regular spacing along stream-wise direction each 5km. 100m  
153 sections are then linked to a section of the 0.1° river network, in order to assign to each section a  
154 synthetic discharge hydrograph. Where the coarse and high resolution river networks do not  
155 overlap, flood points are linked with the closest 0.1° pixel in the upstream direction. Note that  
156 there is not a 1:1 correspondence between 5km and 100m river sections. In particular, some 5km  
157 sections have no related sections in the 100m river network, while others can have more than one.  
158 Figure 2 shows a conceptual scheme of the two river networks. The DEM used to derive the 100m  
159 river network is a component of the River and Catchment Database developed at JRC and  
160 described in Vogt et al., (2007). The same DEM is used also to run flood simulations at 100 m  
161 resolution at each 100m river section using the 2D hydrodynamic model LISFLOOD-FP(Bates  
162 et al., 2010), fed with synthetic hydrographs. Therefore, for every 100m river section we derive  
163 flood maps for the 6 reference return periods.

164 The flood maps related to the same EFAS river section (i.e. pixel of the 5km river network) are  
165 merged together, to identify the areas at risk of flooding because of overflowing from a specific  
166 EFAS river section, and archived in the flood map catalogue. The merging is performed separately  
167 for each return period, in order to relate flooded areas with the magnitude of the flood event.



168  
169  
170  
171  
172

Figure 2: conceptual scheme of the EFAS river network (5 km, squares) with the high resolution network (100m) and river sections (diamonds) where flood simulations are derived. The sections of the two networks related are indicated by the same number. Adapted from Dottori et al. (2015).

### 173 2.2.2 Event-based mapping of flood hazard

174

175 This step of the procedure provides a rapid estimation of the expected flood hazard, using the  
176 database of flood maps described in Section 2.2.1 to translate EFAS discharge forecasts into  
177 event-based flood mapping.

178 At each grid cell, we first identify the median of the ensemble forecast given by the latest EFAS  
179 prediction, and then select the maximum discharge of the median over the full forecasting period  
180 (10 days). The value is compared with the reference long-term climatology to calculate the return  
181 period. In this way, the range of ensemble forecasts is taken as a measure of the probability of  
182 occurrence, while forecast return periods allows to estimate the magnitude of predicted flood  
183 events. Then, predicted streamflow is compared with the local flood protection level, and river  
184 grid cells where the protection level is exceeded are considered to activate the impact assessment  
185 procedure. Flood protection levels are given as the return period of the maximum flood event  
186 which can be retained by the defence measures (e.g. dykes). The map of flood protections used is  
187 based on risk-based estimations for Europe developed by Jongman et al. (2014), integrated, where  
188 available, with the actual level of protection found in literature review or assessed by local  
189 authorities (see Appendix for more details). Note that flood protections are not considered in

190 LISFLOOD-FP simulations because at European scale there is no consistent information about  
191 the location and geometry of flood protection structures (e.g. levees). As such, LISFLOOD-FP  
192 simulations are run as if there were no protection structures.  
193 Selected river cells are reclassified into classes according to the closest return period exceeded  
194 (10, 20, 50, 100, 200, 500 years) and the corresponding flood hazard maps are retrieved from the  
195 catalogue and tiled together. For instance, if the estimated return period is 40 years, the flood map  
196 for 20 years return period is used. Where more maps related to more river sections overlap (see  
197 Section 2.2), the maximum depth value is taken.

### 198 *2.3 Flood impact assessment*

199  
200 After the event-based flood hazard map has been completed, it is combined with the available  
201 information defining the exposure and vulnerability at European scale.

202 The number of people affected is calculated using the population map developed by Batista e  
203 Silva et al. (2012) at 100m resolution. A detailed database of infrastructures produced by Marín  
204 Herrera et al. (2015) is used to compute the extension of the road network affected during the  
205 flood event. The list of major towns and cities potentially affected within the region is derived  
206 from the map of World Cities developed by ESRI (2017). The total extension of urban and built-  
207 up areas (differentiated between residential, commercial and industrial areas) and agricultural  
208 areas is computed using the latest update of the Corine Land Cover for the year 2012 (Copernicus  
209 LMS, 2017).

210 The land use layer also provides the exposure information to compute direct economic losses in  
211 combination with flood hazard variables and flood damage functions, following the approach  
212 developed by Huizinga et al. (2007). More specifically, we use a set of normalized damage  
213 functions to calculate the damage ratio as a function of water depth, spanning from zero (no  
214 damage) to one (maximum damage). The damage ratio is then multiplied by the maximum  
215 damage value, calculated as a function of land use and country's GDP, to calculate actual damage.  
216 Separate damage functions are applied for the land use classes that are more vulnerable to  
217 flooding (residential, commercial, industrial, agricultural). In addition, to account for the variable  
218 value of assets within one country, damage values are corrected considering the ratio between the  
219 gross domestic product (GDP) of regions (identified according to the Nomenclature of Territorial  
220 Units for Statistics (NUTS), administrative level 1) and country's GDP.

221 For countries where specific damage functions could be found in literature, Huizinga et al. (2007)  
222 produced normalized functions based on this national data. In addition, the same authors  
223 elaborated averaged functions to be used for countries without national data, in order to produce  
224 a consistent dataset at European scale. The same approach has been applied in the present study  
225 to elaborate damage curves for countries not included in the original database, like Serbia and  
226 Bosnia-Herzegovina. The complete set of damage functions and the detailed description of the  
227 methodology are available as supplementary data of the recent report by Huizinga et al. (2017).

228 All the results computed during the risk assessment procedure are aggregated using the  
229 classification of EU regions of EUMetNet (the network of European Meteorological Services,  
230 www.meteoalarm.eu). The regions considered are based on the levels 1 and 2 of the NUTS  
231 classification, according to the EU country, with the advantage of providing areas of aggregation  
232 with a comparable extent.

### 233 *3) Benchmarking of the procedure*

234  
235 In order to perform a comprehensive evaluation of the risk assessment procedure, it is important  
236 to evaluate each component of the methodology, namely, streamflow forecasts, event-based flood  
237 mapping, and the impact assessment. The skill of EFAS streamflow forecasts is routinely  
238 evaluated (Pappenberger et al., 2011) while impact assessment was successfully applied by  
239 Alfieri et al. (2016) to evaluate socio-economic impacts of river floods in Europe for the period  
240 1990-2013. Here, the complete procedure is tested using the information collected for the  
241 catastrophic floods of May 2014, which affected several countries in Southeast Europe. In  
242 particular, we focus on the flooding of the Sava River in Bosnia-Herzegovina, Croatia and Serbia.

#### 243 *3.1 The floods in Southeast Europe in May 2014*

244  
245 Exceptionally intense rainfalls from 13 May 2014 onwards following weeks of wet conditions led  
246 to disastrous and widespread flooding and landslides in South-eastern Europe, in particular  
247 Bosnia-Herzegovina and Serbia. In these two countries, the flood events have been reported to be  
248 the worst for over 200 years. Over 60 people lost their lives and more than a million inhabitants  
249 were estimated to be affected, while the estimated damages and losses exceeded 1.1 billion Euro  
250 for Serbia and 2 billion Euro for Bosnia-Herzegovina (ECMWF, 2014; ICPDR and ISRBC,  
251 2015). Critical flooding was also reported in other countries including Croatia, Romania and  
252 Slovakia. Serbia and Croatia requested and obtained access to the EU Solidarity Fund for major  
253 national disasters (EC 2016).

254 According to the technical report issued by the International Commission for the Protection of  
255 the Danube River and the International Sava River Basin Commission (ICPDR and ISRBC,  
256 2015), the flood events were particularly severe in the middle-lower course of the Sava River and  
257 in several tributaries. The discharge measurements and estimations carried out between 14 and  
258 17 May indicated that the peak flow magnitude exceeded the 500 years return period both in the  
259 Bosna and Kolubara rivers and in part of the Sava River downstream of the confluence with  
260 Bosna. Discharges above 50 years were observed in the Una, Vrbas, Sana and Drina rivers (Figure  
261 3).

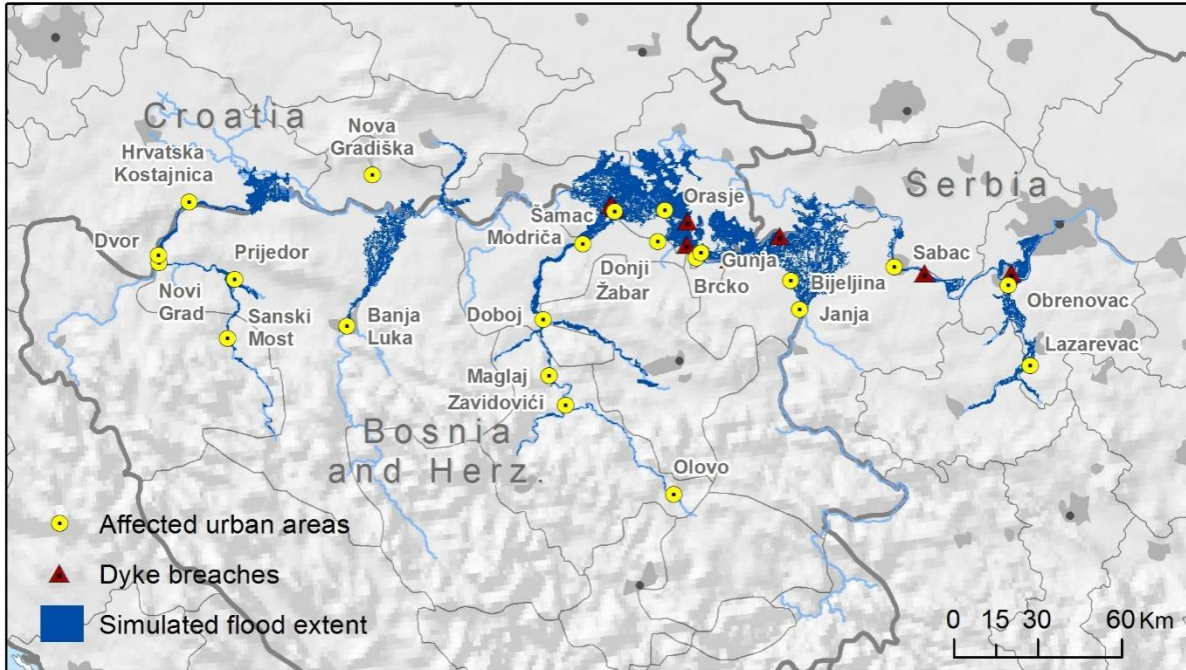




262  
 263 *Figure 3. Reconstruction of return period of peak discharges in Sava River basin (source:*  
 264 *ICPDR and ISRBC, 2015).*  
 265

266 The lower reach of the Sava was less heavily affected because upstream flooding reduced peak  
 267 discharges and hydraulic operations on the Danube hydraulic structures reduced water levels in  
 268 the Danube (ICPDR and ISRBC, 2015). Due to the extreme discharges, multiple dyke breaches  
 269 occurred along the Sava River, and severe flooding occurred at the confluence of tributaries like  
 270 Bosna, Drina and Kolubara (Figure 4). In many areas, dykes were reinforced and heightened  
 271 during the flood event to withstand the peak flow; also, additional temporary flood defences were  
 272 built to prevent further flooding, and drains were dug to drain flooded areas more quickly. Other  
 273 rivers in the area experienced severe flood events, such as the tributaries of the Danube Velika  
 274 Morava and Mlava, in Serbia.

275 Table 1 reports a summary of flood impacts at national level for Bosnia-Herzegovina, Croatia and  
 276 Serbia, retrieved from different sources.



277  
 278 *Figure 4. Reconstruction of affected urban areas and dyke failure locations along the Sava River*  
 279 *(sources: UNDAC, 2014; ICPDR and ISRBC, 2015). The flood extent of the reference*  
 280 *simulation with the proposed procedure is also shown (see Section 3.2).*  
 281

	Flooded area (km <sup>2</sup> )	Casualties <sup>(1)</sup>	Affected population <sup>(1)</sup>	Evacuated population <sup>(1)</sup>	Economic impact (M€)
Bosnia-Herzegovina	266.3 <sup>(1)</sup> ; 831 <sup>(2)</sup>	25	1.6 million	90000	2040
Croatia	53.5 <sup>(1)</sup> ; 110 <sup>(3)</sup> ; 210 <sup>(4)</sup>	3	38000	15000	300
Serbia	22.4 <sup>(1)</sup> ; 221 <sup>(3)</sup> ; 350 <sup>(5)</sup>	51	1 million	32000	1530 <sup>(1)</sup>

282  
 283 *Table 1. Summary of flood impacts at national level. Figures have been retrieved from the*  
 284 *following sources: 1- ICPDR and ISRBC (2015); 2- Bosnia-Herzegovina Mina Action Center*  
 285 *(BHMACH, Bajic et al 2015); 3- Copernicus EMS Rapid Mapping Service; 4- Wikipedia (2016);*  
 286 *5- GeoSerbia geoportal (2016).*

### 287 **3.2 Evaluation of the flood hazard mapping procedure**

288  
 289 We considered in our analysis the river network of the Sava River basin, where some of the most  
 290 affected areas are located and for which detailed information is available from various reports.

291 To evaluate the skill of the flood hazard mapping procedure, we used observed flood magnitudes  
292 (Figure 3) to identify the return period of peak discharges and thus select the appropriate flood  
293 maps. In addition, we used the information on flood protection level and dyke failures to select  
294 only those river sections where flooding actually occurred, either because of defence failures or  
295 exceeding discharge. The resulting flood hazard map will be named from now on as “reference  
296 simulation”. Such a procedure excludes the uncertainty due to the hydrological input from the  
297 analysis, focusing on the evaluation of the flood hazard mapping approach alone. In other words,  
298 the test can be seen as an application of the procedure in case of a single, deterministic and  
299 “perfect” forecast. The resulting inundation map is displayed in Figure 4.

300 It is important to note that a margin of uncertainty remains because of the emergency measures  
301 taken during the event. In several river sections of the Sava River, the flood defences were actually  
302 able to withstand discharges well above their design value, thanks to timely emergency measures  
303 such as the heightening and strengthening of dykes. Moreover, the preparation of temporary flood  
304 defences in the floodplains helped to protect some areas which would have been otherwise  
305 flooded. A further issue of the methodology is that, where flood protections are exceeded,  
306 flooding can occur on both river banks, while in case of dyke failure flooding is usually limited  
307 to one side where protection level is lower. This has not been corrected and therefore the results  
308 are affected by this limitation.

309 The flood events in the Sava River have been mapped by several agencies and institutions using  
310 both ground observations and satellite imagery (see UN SPIDER (2014) for a complete list). The  
311 most comprehensive flood maps were developed by the Copernicus Emergency Management  
312 System (EMS) using Sentinel-1 data (EMS, 2014), and by NASA using MODIS Aqua (UN  
313 SPIDER, 2014). For Serbia, the Republic Geodetic authority has acquired and processed further  
314 satellite images, which are available on the geoportal GeoSerbia (2016).

315 Despite this large amount of data sources available, the evaluation of the simulated flood extent  
316 is not straightforward. All the available images have been acquired during the flood recession  
317 (from 19 May onwards), while flood peaks were observed between 15 and 17 May. Therefore,  
318 several areas which have been reported as flooded in the available documentation are not included  
319 in the detected flood footprints, which results in a significant difference between satellite-detected  
320 and reported flood extent from ground surveys (see Table 1). On the other hand, EMS satellite  
321 maps are designed to produce a low rate of false positive errors, therefore they can be considered  
322 as a “lower limit” for the real flood extent. Finally, it has to be considered that the available  
323 sources of information report for each country different extents of flooded area, as can be seen in  
324 Table 1.

325 In order to take into account these issues, we first compare the total simulated and reported flood  
326 extent at country level, calculating overestimation (or underestimation) rates against all the  
327 available reported data. Then, we evaluate the agreement between satellite-derived and simulated  
328 flood extent considering those areas in the Sava River basin affected by the flood event and where  
329 satellite maps from Copernicus were available. Areas were grouped considering the main source  
330 of flooding, either a tributary (e.g. Bosna River) or the Sava River. For the Sava River, we

331 considered two separate sectors because of the large extent of the flooded areas, and because flood  
332 extent was not continuous. The agreement is evaluated using the hit ratio H (Alfieri et al., 2014b),  
333 defined as:

334

$$335 \quad H = (Fm \cap Fo)/(Fo) \times 100 \quad (1)$$

336

337 where  $Fm \cap Fo$  is the area correctly predicted as flooded by the model, and  $Fo$  is the total  
338 observed flooded area. Note that we did not consider indices to evaluate false hit ratios because,  
339 as previously discussed, we know that the available satellite flood maps underestimated the actual  
340 flood extent. Consequently, false alarm ratio scores would be low without being supported by  
341 reliable observations, giving an incorrect view of the performance. As a further element, we  
342 compare the number of urban areas (cities, towns and villages) which were reported as flooded  
343 by UNDAC (2014) and ICPDR and ISRBC (2015).

### 344 *3.2 Evaluation of forecast-based flood hazard maps*

345

346 To evaluate the overall performance of forecast-based flood hazard mapping, we considered the  
347 EFAS forecasts issued on 12 and 13 May for the Sava river basin, that is, immediately before the  
348 occurrence of first flood events on 14 May. We first applied the standard procedure described in  
349 Section 2 to derive peak discharges, estimated return periods and flood maps using the median of  
350 the EFAS ensemble forecasts. To provide a more complete overview of risk scenarios, we also  
351 applied the procedure considering the 25 and 75 percentiles of discharge in the ensemble  
352 forecasts. As a first step, we evaluate EFAS forecast by comparing forecast and observed return  
353 periods. Then, forecast-based flood hazard maps are evaluated against the reference simulation,  
354 comparing the river sectors and the urban areas (or municipalities) at risk of flooding. Note that  
355 we selected the reference simulation as benchmark because it represents the best result achievable  
356 in case of a perfect forecast. Conversely, we did not carried out a comparison against observation-  
357 based flood maps, because they incorporate the effect of defence failures or strengthening, which  
358 could be considered in forecast-based maps only as hypothetical scenarios.

### 359 *3.3 Evaluation of impact assessment*

360

361 Inundation maps derived from the reference simulation and flood forecasts have been used to  
362 compute flood impacts in terms of number of affected people, affected major towns and cities,  
363 and economic damage.

364 The results are compared with the available impact estimations both at national and local level.  
365 For Serbia and Bosnia-Herzegovina, the national figures reported in Table 1 are referred to the  
366 total impact given by river floods, landslides and pluvial floods, therefore they cannot be directly  
367 compared with methodology results. As such, the comparison has been done only for Croatia and

368 for a number of municipalities (e.g. Obrenovac in Serbia) where impacts can be attributed to river  
 369 flooding alone.

370 The figures of affected population computed with the reference simulation are also useful to test  
 371 the reliability of the population map used as exposure dataset. Similarly, damage estimations  
 372 provide an indication of the reliability of depth-damage curves for the study area.

373 As done for the flood hazard maps, forecast-based risk estimations are evaluated against the  
 374 results from the reference simulation, comparing both population and damage figures. Note that  
 375 other variables produced by the operational procedure (e.g. roads affected, extent of flooded urban  
 376 and agricultural areas) could not be tested due to the lack of observed data and therefore are not  
 377 discussed here. To add a further term of comparison, affected population has been computed using  
 378 Copernicus-EMS flood footprints.

#### 379 **4) Results and discussions**

380  
 381 The results of the evaluation exercise are shown and discussed separately for each component of  
 382 the procedure.

#### 383 **4.1 Flood hazard mapping**

384  
 385 Table 3 reports the observed flood extent data from available sources and the simulated extent  
 386 derived from the reference simulation (i.e. the mapping procedure applied on discharge  
 387 observations). The ratios between simulations and observations are also included. Table 4 reports  
 388 the scores of the hit ratio H for the considered flooded sectors, together with a comparison of  
 389 towns flooded according to simulations and observation.  
 390

	Flood extent (km <sup>2</sup> )			
<b>Country</b>	Reference simulation	Satellite	Reported by ICPDR-ISRBC	Reported (other sources)
<b><i>Bosnia - Herzegovina</i></b>	995	339	266.3 <sup>(1)</sup>	831 <sup>(2)</sup>
<b><i>Croatia</i></b>	919 (319)	110	53.5 <sup>(1)</sup>	>210 <sup>(3)</sup>
<b><i>Serbia</i></b>	582	221	22.4 <sup>(1)</sup>	>350 <sup>(4)</sup>
	Extent ratio			
<b>Country</b>	Reference simulation	Satellite	Reported by ICPDR-ISRBC	Reported (other sources)
<b><i>Bosnia - Herzegovina</i></b>	1	0.34	0.27	0.84
<b><i>Croatia</i></b>	1	0.12 (0.34)	0.06 (0.17)	>0.23 (0.66)
<b><i>Serbia</i></b>	1	0.38	0.04	>0.60

391

392 *Table 3. Comparison of observed and simulated flood extent data at country scale. Satellite*  
 393 *flood extent is referred to Copernicus EMS maps. Values between parentheses for Croatia are*  
 394 *referred to a modified simulation, as explained in the text. Reported flood extent has been*  
 395 *retrieved from the following sources: 1- ICPDR and ISRBC (2015); 2- Bosnia-Herzegovina*  
 396 *Mina Action Center (BHMAC, Bajic et al 2015); 3- Wikipedia (2016); 4 –GeoSerbia geoportal*  
 397 *(2016).*  
 398

<b>Affected areas</b>	<b>Hit ratio</b>	<b>EMS flooded area (km<sup>2</sup>)</b>	<b>Affected towns and cities</b>
Bosna River	90.6%	58.46	Maglaj, Doboj, Modriča
Sava River between confluences with Bosna and Drina	63.9%	134.76	Orašje, Šamac, Donji Žabar, Brcko, Gunja, (Zupanja), Bijeljina
Sava River between confluences with Drina and Kolubara	83.7%	405.43	Sabac, Obrenovac, Lazarevac
<b>Total</b>	<b>79.9%</b>	<b>598.65</b>	

399 *Table 4. Scores of the hit ratio H for the considered flooded sectors, and affected towns and*  
 400 *cities. Names between parentheses refer to towns and cities wrongly predicted as flooded,*  
 401 *otherwise towns and cities have been correctly predicted as flooded.*  
 402

403 As expected, the simulated flood extent is significantly larger in all the cases than the satellite  
 404 extent (see Table 3), given the delay between flood peaking time and time of image acquisition  
 405 mentioned in Section 3.2. Flood extent indicated in the ICPDR and ISRBC report is also  
 406 consistently lower than values from both simulated and satellite maps.  
 407 Simulated and reported extent are instead more comparable when considering data reported by  
 408 other sources. For Bosnia-Herzegovina, the simulated value is close to the reported flood extent  
 409 published in the report by Bajic et al. (2015). For Serbia, the flooded area detected from  
 410 GeoSerbia satellite maps is smaller than the simulation, but it has to be considered that these maps  
 411 have the same problem of delayed image acquisition mentioned for Copernicus maps. For Croatia,  
 412 the flood mapping methodology is largely overestimating both the satellite-based and reported  
 413 flood extents. The main reason is that flooding on the left side of Sava was limited due to the  
 414 reinforcing of river dykes in the area close to the city of Zupanja, which could withstand the  
 415 reported 500 years return period discharge despite having been designed for a 1 in 100 year event.  
 416 In fact, all the left bank of Sava in this area was reported as an area at risk in case of a flood  
 417 defence failure, and only the emergency measures taken prevented more severe flooding (ICPDR  
 418 and ISRBC, 2015). Therefore we performed an additional flood simulation excluding any failure  
 419 on the river left bank between the Bosna confluence and Zupanja, and in this case we found a  
 420 total flood extent of 319 km<sup>2</sup>. Even if this estimate still exceeds reported flood extent (Wikipedia,  
 421 2016), it has to be considered that this figure is referred only to the Vukovar-Srijem county, which  
 422 was the most affected area, therefore the total affected area in all the country was probably larger.

423 Regarding Table 4, the scores of the H index indicate that the mapping procedure correctly  
 424 detected most of the flooded areas, although with the partial exception of the lower Sava area. In  
 425 particular, the great majority of towns reported to have been flooded are correctly detected by the  
 426 simulations, with only few false alarms (e.g. the already mentioned Zupanja).  
 427 When looking at the results it is important to keep in mind the limitations of the procedure. As  
 428 mentioned in Section 2.3, the mapping procedure is able to reproduce only maximum flood  
 429 depths, and the dynamic of the flood event is not taken into account. This means that processes  
 430 like flood wave attenuation due to inundation occurring upstream cannot be simulated, and  
 431 possible flood mitigation measures taken during the event are not considered as well.  
 432 Furthermore, due to the coarse resolution (100m) of the DEM used in flood simulations, flood  
 433 simulations do not include small scale topographic features like minor river channels, dykes and  
 434 road embankments.

#### 435 4.2 Flood impact assessment

436  
 437 Tables 5 summarizes reported and estimated impacts on population, based on both the reference  
 438 simulation and Copernicus satellite maps, for the 3 countries affected by floods in the Sava basin.  
 439 Tables 6 reports simulated and reported impacts on population for a number of administrative  
 440 regions where impacts can be attributed to floods only. For evaluating the performance of impact  
 441 assessment, we take into consideration only Table 6, because national estimates in Table 5  
 442 consider also people displaced by landslides and pluvial floods not simulated in EFAS.  
 443 Note that in both tables we compare simulated impacts with figures of evacuated population  
 444 because reported estimates of affected population included also people affected by indirect effects  
 445 like energy shortage and road cuts. Note also that the figures of evacuated population are not  
 446 equivalent to directly affected population (i.e. whose houses were actually flooded). In some  
 447 areas, evacuation was taken as a precautionary measure, even if flooding did not eventually occur.  
 448

Country	Evacuated population (reported)	Affected population (satellite)	Affected population (simulated)
Bosnia-Herzegovina	90.000	51.010	215.200
Croatia	27.260	5.760	57.000
Serbia	32.000	13.700	29.800

449 *Table 5. Comparison of evacuated population (reported) and affected population estimated from*  
 450 *satellite and simulations in Bosnia-Herzegovina, Croatia and Serbia (source: ICPDR and*  
 451 *ISRBC, 2015).*

Administrative area	Country	Evacuated population (reported)	Affected population (simulated)

Obrenovac municipality	Serbia	> 25000	17600
Brcko district	Bosnia-H.	1200	1700
Brod-Posavina county	Croatia	13700	12800
Osijek-Baranja county	Croatia	200	1300
Sisak-Moslavina county	Croatia	2400	3300
Požega-Slavonija county	Croatia	2300	1500
Vukovar-Srijem county	Croatia	8700	39200

453

454 *Table 6. Comparison of evacuated population (reported) and affected population (simulated) in*  
455 *administrative areas in Bosnia-Herzegovina, Croatia and Serbia (source: ILO, 2014; ICPDR*  
456 *and ISRBC, 2015; Wikipedia, 2016)*

457

458 As can be seen, differences between results and reported figures are in the order of hundreds,  
459 suggesting that the procedure is able to provide a general indication of the impact on population,  
460 but with a limited precision where impacts are small, as in the case of the Osijek-Baranja county.  
461 However, differences are larger for the Vukovar-Srijem county in Croatia, and the Obrenovac  
462 municipality in Serbia. For the former, this is due to the overestimation of flooded areas discussed  
463 in Section 4.1. If dyke failures are not included in the simulation for this county, the affected  
464 population is reduced to 8600 people, extremely close to the reported figure. The underestimation  
465 in the Obrenovac municipality may indicate that flood simulations are less reliable for urban  
466 areas, even if estimated figures still depict a major impact on the city. In fact, the DEM used in  
467 the simulations is mostly based on elevation data from the Shuttle Radar Topography Mission  
468 (SRTM) which is known to be less accurate in urban and densely vegetated areas (Sampson et  
469 al., 2015).

470 For flood impacts related to monetary damage, the simulations for Croatia indicate a total damage  
471 of 653 M€, against a reported estimate of 298 M€. However, if the already mentioned  
472 overestimation of flooded areas is considered, then the estimate decreases to 190 M€. The  
473 difference is relevant but still within the usual range of uncertainty of damage models (Wagenaar  
474 et al., 2016). As already mentioned, damage figures for Serbia and Bosnia-Herzegovina could not  
475 be used because available estimates aggregate damages from landslides and river and pluvial  
476 flooding.

477 The observed underestimation has to be evaluated considering the limitations of both observed  
478 data and damage assessment methodology. On one hand, the damage functions available for  
479 Croatia are not specifically designed for the country, as discussed in Section 2.3. Also, estimated  
480 damages include only direct damage to buildings, while infrastructural damage is only partially  
481 accounted for (e.g. damage to the dyke system). On the other hand, official estimates are affected  
482 by the absence of clear standards for loss assessment and reporting (Corbane et al., 2015; IRDR,  
483 2015) and can strongly deviate from true extents and damages. Thielen et al. (2016) observed  
484 that reported losses are rarely complete and that it may require years before reliable loss estimates  
485 are available for an event.



486 **4.3EFAS forecasts**

487

488 Table 7 illustrates return periods of peak discharge derived from 12 and 13 May forecasts for the  
 489 main rivers of the Sava basin, visible in Figure 3. Simulations are compared against values  
 490 reported by ICPDR and ISRBC (2015).

491

River	12/5 25p.	12/5 50p.	12/5 75p.	13/5 25p.	13/5 50p.	13/5 75p.	Reported
Return period forecast (years)							
Una	< 5	< 5	< 5	< 5	< 5	< 5	50
Sana	< 5	< 5	< 5	< 5	5-10	5-10	50
Bosna	< 5	5-10	10-20	5-10	20-50	50-100	500
Vrbas	< 5	5-10	10-20	5-10	10-20	20-50	100
Drina	< 5	< 5	5-10	<5	5-10	10-20	50
Kolubara	10-20	20-50	100-200	20-50	50-100	>200	500
Sava (upper reach)	< 5	< 5	< 5	< 5	< 5	< 5	20
Sava (middle reach)	< 5	< 5	< 5	<5	5-10	5-10	500
Sava (lower reach)	5-10	5-10	10-20	10-20	10-20	20-50	100

492

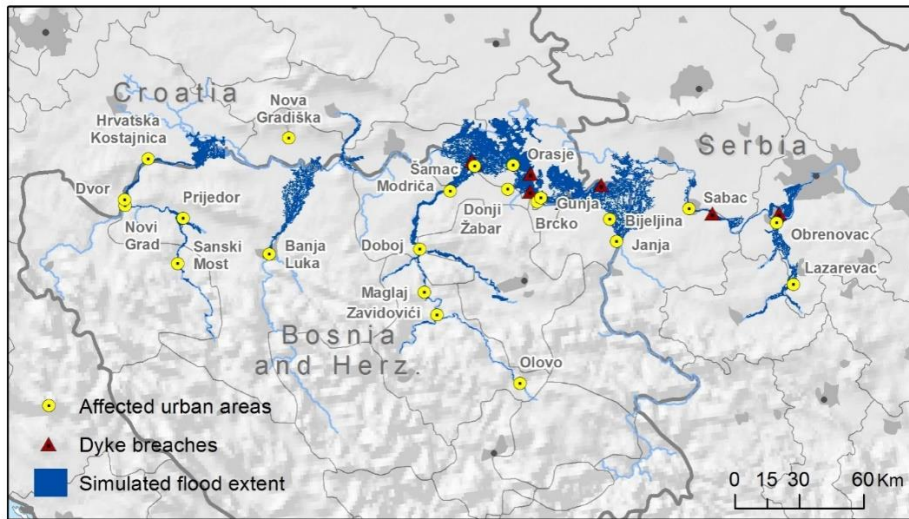
493 *Table 7. Comparison of forecast and observed return periods in the main rivers of the Sava*  
 494 *Basin. The Sava River has been divided in 3 sectors. Upper: up to confluence with the Bosna*  
 495 *River; middle: between the confluences with Bosna and Drina rivers; lower: from the*  
 496 *confluence with the Drina River to the confluence into the Danube River.*

497

498 Results show that forecasts for 12 May are significantly far from observations even considering  
 499 the 75<sup>th</sup> percentile, with the exception of Kolubara River. The performance improves for the 13  
 500 May, when the magnitude of predicted discharges indicates a major flood hazard in most of the  
 501 considered rivers, although with a general underestimation especially in the Una, Sana and in the  
 502 upper and middle reaches of the Sava River. However, it has to be considered that peak flow  
 503 timing was rather variable across the Sava river basin, due to its extent. While in the Kolubara  
 504 river the highest discharges occurred on 14 and 15 May, peak flows in other tributaries were  
 505 reached later (between 14<sup>th</sup> and 16<sup>th</sup> for Bosna River, on 16<sup>th</sup> for Drina, on 17<sup>th</sup> for Sana River),  
 506 and on the main branch of the Sava River the flood peaks occurred after 17 May. Thus, in a  
 507 hypothetical scenario where EFAS risk forecast were routinely used for emergency management,  
 508 on one hand there would have been still time to update flood forecasts. On the other hand, the  
 509 forecast released on 13 May would have given to emergency responders a warning time of at least  
 510 2 days to plan response measures in several affected areas, chiefly in the Kolubara and Bosna  
 511 basins.

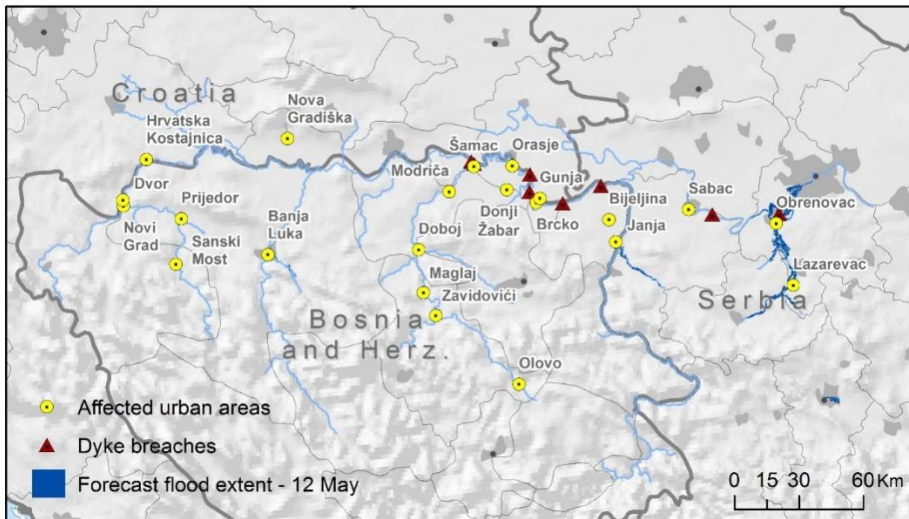
512 Figure 5 shows the inundation maps derived using the median of ensemble streamflow forecasts  
 513 issued on 12 and 13 May (that is, the standard procedure adopted for the operational procedure).

514



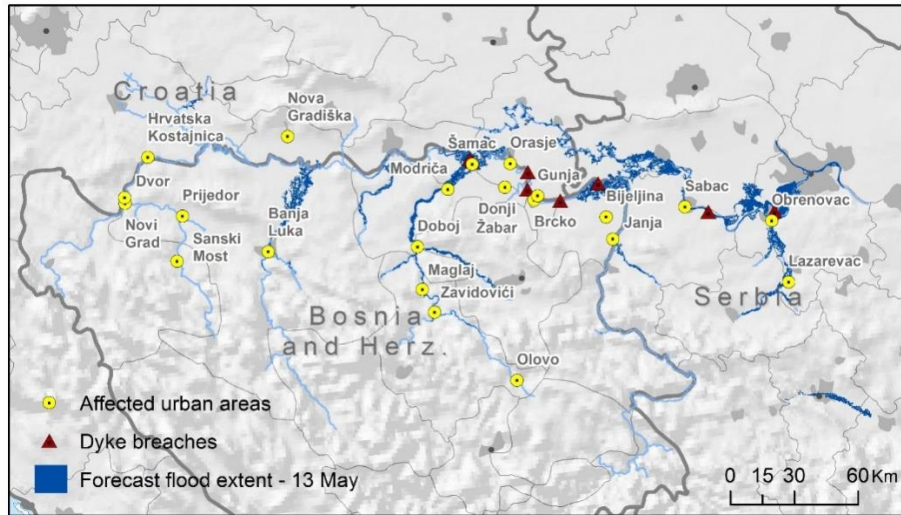
515

a



516

b



517  
 518 *Figure 5. Simulated flood extent based on reference simulation (a), 12 May (b) and 13 May*  
 519 *forecasts (c), with location of reported flooded urban areas and dyke failures.*

520  
 521 In addition, Table 8 illustrates the outcomes of impact forecasts, compared to impacts obtained  
 522 from the reference simulation. For both dates, we considered predicted maximum streamflow  
 523 values based on the 25<sup>th</sup>, 50<sup>th</sup> and 75<sup>th</sup> percentiles of the ensemble forecast. All of estimations  
 524 are computed taking into account local flood protection levels.

525

Country	12/5 25p.	12/5 50p.	12/5 75p.	13/5 25p.	13/5 50p.	13/5 75p.	Ref. Sim.
flood extent (km <sup>2</sup> )							
Bosnia-Herz.	0	5	196	110	406	494	995
Croatia	0	0	100	54	95	135	919
Serbia	91	187	385	241	562	664	582
affected population							
Bosnia-Herz.	0	5,230	2,046	20,600	95,530	117,280	215,180
Croatia	0	0	3,600	1,940	2'780	4,480	57,050
Serbia	2,790	6,010	15,120	11,150	25,950	32,660	29,760
economic damage (million €)							
Bosnia-Herz.	0	10	36	28	245	342	378
Croatia	0	0	41	13	22	37	653
Serbia	14	31	92	77	197	249	141

526  
 527 *Table 8. Comparison of forecast flood impacts with the reference simulation.*

528  
 529 Figures in Table 8 allows to further expand the analysis done on predicted flood magnitudes, and  
 530 illustrates the evolution of flood risk depicted by EFAS ensemble forecasts. As can be seen, the

531 impact estimate derived from 12 May forecast was indicating a limited risk with the exception of  
532 Serbia, even if the figures for the 75<sup>th</sup> percentile already indicated the possibility of more relevant  
533 impacts. The overall risk increases with 13 May forecast, with severe and widespread impacts  
534 associated to the ensemble forecast median, even though for Bosnia- Herzegovina and especially  
535 Croatia there is still a significant underestimation with respect to reference simulation. A further  
536 important result is that the location of forecast flooded areas is mostly consistent with the  
537 reference simulation shown in Figure 3, with several urban areas already at risk of flooding in the  
538 map based on 13 May forecast (Figure 6).  
539 In a hypothetical scenario, these results would have provided emergency responders with valuable  
540 information to plan adequate countermeasures, based on the expected spatial and temporal  
541 evolution of flood risk. A more detailed discussion on these topics is reported in Section 4.4.

#### 542 *4.4 Discussion*

543  
544 As discussed in the Introduction, the availability of a risk forecasting procedure able to transform  
545 hazard warning information into effective emergency management (i.e. risk reduction) (Molinari  
546 et al., 2013), opens the door to a wide number of new applications in emergency management and  
547 response. However, to better understand the limitations of the procedure, as well as its potential  
548 for future applications, some considerations have to be made.

549 First, it is important to remember that EFAS is a continental scale system which is mainly  
550 designed to provide additional information and support the activity of national flood emergency  
551 managers. Therefore, the practical use of risk forecasts to activate emergency measures would  
552 need to be discussed and coordinated with services and policy makers at local level.

553 Second, the new procedure needs to undergo an accurate uncertainty analysis before risk forecasts  
554 can effectively be used for emergency management. While a detailed analysis is beyond the scope  
555 of this paper, to this end, we recently started to evaluate the performance of the procedure for the  
556 flood events recorded in the EFAS and Copernicus EMS databases.

557 Another point to consider is the approach chosen to assess flood risk. In the current version of the  
558 procedure, we produce a single evaluation based on the ensemble forecast median to provide a  
559 straightforward measure of the flood risk resulting from the overall forecast. A more rigorous  
560 approach would require to analyse all relevant flood scenarios resulting from EFAS forecasts and  
561 estimate their consequences together with the conditional probability of occurrence, given the  
562 range of ensemble forecast members and the forecast uncertainty (Apel et al., 2004). While such  
563 a framework would enable a cost-benefit analysis of response measures in an explicit manner, it  
564 would also require to evaluate the consequences of wrong forecasts, like missing or  
565 underestimating impending events, or issuing false alarms (Molinari et al., 2013; Coughlan et al.,  
566 2016). Given the difficulty of setting up a similar framework at European scale, during the initial  
567 period of service EFAS risk forecast will be used to plan “low regret” measures like satellite  
568 monitoring and warning of local emergency services. For instance, we are currently evaluating  
569 the use of EFAS risk forecast to trigger satellite rapid flood mapping through Copernicus EMS,

570 with the aim of improving response time and detection of flooded areas. More demanding  
571 measures (e.g. monitoring and strengthening of flood defences in endangered river sections, road  
572 closures in areas at risk, deployment of emergency services, evacuation planning of endangered  
573 people), could instead be put in place upon confirmation from local flood monitoring systems.  
574 When designing the structure and output of risk assessment, it has to be considered that the type  
575 and amount of information provided must be based on users' requests. As a matter of fact,  
576 different end users may be interested in different facets of flood impact (Molinari et al., 2014),  
577 but at the same time it is important to avoid information overload during emergency management.  
578 Again, finding a compromise requires a close collaboration with the user community.  
579 For instance, damage estimation has been included in the impact assessment upon request of  
580 EFAS end users, despite the known limitations of the damage functions dataset, in particular the  
581 absence of country-specific damage functions for the majority of countries in Europe. From this  
582 point of view, the case study described in this work is representative of the level of precision that  
583 may be achievable in these countries. Future improvements can be possible with the availability  
584 of detailed, country-specific damage reports at building scale (i.e. reporting hazard variables and  
585 the consequent damage for different building categories) that would allow to derive specific  
586 damage functions.  
587 For the same reasons, human safety and the protection of human life have not been addressed in  
588 this study, despite their importance in emergency management. The scale of application of the  
589 EFAS risk assessment is not compatible with risk models for personal safety based on precise  
590 hydrodynamic analysis, like the one presented by Arrighi et al. (2016), whereas probabilistic risk  
591 methods (e.g. de Bruijn et al., 2014) and the use of mortality rates calculated from previous flood  
592 events (e.g. Tanoue et al., 2016) are more feasible of integration and could be tested for next  
593 releases of the risk forecasting procedure.

594

## 595 *5) Conclusions and next developments*

596

597 This paper presents the first application of a risk forecasting procedure which is fully integrated  
598 within a continental scale flood early warning system. The procedure has been thoroughly tested  
599 in all its components to reproduce the Sava River basin floods in May 2014, and the results  
600 demonstrate the potential of the proposed approach.

601 The rapid flood hazard mapping procedure applied using observed river discharges was able to  
602 identify flood extent and flooded urban areas, while simulated impacts were comparable with  
603 observed figures of affected population and economic damage. The evaluation was complicated  
604 on one hand by the scarcity of reported data at local scale, and on the other hand by the  
605 considerable differences in impacts reported by different sources, especially regarding flood  
606 extent. This is a well know problem in flood risk literature, due to the fact that existing standards  
607 for impact data collection and reporting are still rarely applied (Thieken et al., 2016). Therefore,

608 further improvements of impact models will require the availability of impact data complying  
609 with international standards (Corbane et al., 2015; IRDR, 2015).

610 The application using EFAS ensemble forecasts enabled to identify areas at risk with a lead time  
611 ranging from 1 to 4 days, and to correctly evaluate the magnitude of flood impacts, although with  
612 some inevitable limitation due to difference between simulated and observed streamflow. When  
613 evaluating the outcomes, it is important to remember that, even in case of a risk assessment based  
614 on “perfect” forecasts and modelling, simulated impacts will always be different from actual  
615 impacts. As we have shown in the test case of the floods in the Sava River basin, unexpected  
616 defence failures can occur for flow magnitudes lower than the design level, thus increasing flood  
617 impacts. On the other hand, flood defences might be able to withstand greater discharges than the  
618 design level, and emergency measures can improve the strength of flood defences or creating new  
619 temporary structures. As such, forecast-based risk assessment should be regarded as plausible risk  
620 scenarios that can provide valuable information for local, national and international authorities,  
621 complementing standard flood warnings. In particular, the explicit quantification of impacts  
622 opens the road to a more effective use of early warning information in emergency management,  
623 allowing to evaluate costs and benefits of response measures.

624 After a testing phase started in September 2016, since March 2017 the procedure is fully  
625 operational within the EFAS modelling chain. Besides the version currently in use and described  
626 in this paper, we plan to test a number of modifications and alternative approaches for hazard  
627 mapping and risk assessment will be tested in the near future. Currently, inundation forecasting  
628 is computed using the median of EFAS daily ensemble streamflow forecasts, but in principle the  
629 methodology can easily more detailed risk evaluations taking into account less probable but  
630 potentially more severe flood scenarios predicted by ensemble members (see the application  
631 described this paper). Furthermore, additional risk scenarios can be produced by considering the  
632 failure of local flood defences, or replacing EFAS flood hazard maps with official hazard maps  
633 developed by national authorities, where available. The influence of lead time on flood  
634 predictions could also be assessed, for instance by setting a criterion based on forecasts  
635 persistence over a period to trigger the release of impact forecasts. All these alternatives will be  
636 tested in collaboration with the community of the EFAS users, to maximize the value of the  
637 information provided and avoid information overload which can be difficult to manage in  
638 emergency situations.

639 A further promising application that is being tested is the use of inundation forecast to activate  
640 rapid flood mapping from satellites, exploiting the Copernicus Emergency Mapping Service of  
641 the European Commission.

642 Finally, the proposed procedure will also be incorporated into the Global Flood Awareness  
643 System (GloFAS), which would allow to establish a near-real time flood risk alert system at global  
644 scale.

645

646

647

## 648 *Acknowledgements*

649

650 This work has been partially funded by the COPERNICUS programme and an administrative  
651 arrangement with the Directorate General Humanitarian Aid and Civil Protection (DG ECHO) of  
652 the European Commission.

653 The authors would like to thank Jutta Thielen and Vera Thiemig for their valuable suggestions on  
654 early versions of the manuscript.

655

## 656 *Appendix*

### 657 *Update of flood protection maps for Europe*

658

659 We include in Table S1a list of the updates to the flood protection level map developed by  
660 Jongman et al. (2014), in use for the risk assessment procedure. The table shows the rivers where  
661 values have been updated, the geographic location (in some cases, the protection values has been  
662 modified only at specific locations along the river), previous and updated values, and the source  
663 of information (either the report .Protection values are expressed in years of the event return  
664 period.

665 In addition to the modifications in Table S1, it is planned to further update the EFAS database  
666 using the global flood protection layer FloPROS (Scussolini et al., 2016).

667

River	Region, Country	Previous values	Updated values	Reference
Sava	Croatia, Serbia, Bosnia-Herzegovina,	Not included -20	100	ISRBC, 2014
Drina	Bosnia-Herzegovina,	Not included	50	ISRBC, 2014
Una, Vrbas, Sana, Bosna	Bosnia-Herzegovina, Croatia	Not included-10	30	ISRBC, 2014
Kolubara	Serbia	Not included	50	ISRBC, 2014

668 *Table S1. Update of the flood protection level map developed by Jongman et al. (2014), in use for*  
669 *the risk assessment procedure.*

670

671 *Bibliography*

672

673 Alfieri L., Pappenberger F., Wetterhall F., Haiden T., Richardson D., Salamon P., 2014a.  
674 Evaluation of ensemble streamflow predictions in Europe, *Journal of Hydrology*, 517, 913-922

675 Alfieri, L., Salamon, P., Bianchi, A., Neal, J., Bates, P.D., Feyen, L., 2014b. Advances in pan-  
676 European flood hazard mapping, *Hydrol. Process.*, 28 (18), 4928-4937, doi:10.1002/hyp.9947.

677 Alfieri, L., Feyen, L., Salamon, P., Thielen, J., Bianchi, A., Dottori, F., and Burek, P.:  
678 Modelling the socio-economic impact of river floods in Europe, *Nat. Hazards Earth Syst. Sci.*,  
679 16, 1401-1411, doi:10.5194/nhess-16-1401-2016, 2016.

680 Apel H., Thielen A. H., Merz B., Blöschl B., 2004. Flood risk assessment and associated  
681 uncertainty. *Nat. Hazards Earth Syst. Sci.* 4 (2), 295-308.

682 Arrighi. C., Oumeraci, H., Castelli, F., 2017. Hydrodynamics of pedestrians' instability in  
683 floodwaters. *Hydrol. Earth Syst. Sci.*, 21, 515–531, 2017, doi:10.5194/hess-21-515-2017.

684 Bates P.D., Horritt M.S., and Fewtrell T.J. (2010). A simple inertial formulation of the  
685 shallow water equations for efficient two-dimensional flood inundation modelling. *Journal of*  
686 *Hydrology*, 387, 33–45.

687 Batista e Silva F., Gallego J., and Lavalle C. (2013). A high-resolution population grid map  
688 for Europe. *Journal of Maps*, 9 (1), 16-28.

689 Burek, P., Knijff van der, J., Roo de, A., 2013. LISFLOOD, Distributed Water Balance and  
690 Flood Simulation Model Revised User Manual 2013. Publications Office, Luxembourg.

691 Cloke, H., Pappenberger, F., Thielen, J. and Thiémig, V. (2013) Operational European Flood  
692 Forecasting, in *Environmental Modelling: Finding Simplicity in Complexity*, Second Edition (eds  
693 J. Wainwright and M. Mulligan), John Wiley & Sons, Ltd, Chichester, UK. doi:  
694 10.1002/9781118351475.ch25.

695 Copernicus Emergency Management Service - Mapping. Institute for the Protection and  
696 Security of the Citizen (IPSC), European Commission, Joint Research Centre (JRC). Accessed  
697 November 12, 2014. <http://emergency.copernicus.eu/>.

698 Copernicus Land Monitoring Service. Corine Land Cover. [http://land.copernicus.eu/pan-](http://land.copernicus.eu/pan-european/corine-land-cover)  
699 [european/corine-land-cover](http://land.copernicus.eu/pan-european/corine-land-cover) (accessed 12-2-2017).

700 Corbane, C., de Groeve, T., and Ehrlich, D.: Guidance for Recording and Sharing Disaster  
701 Damage and Loss Data – Towards the development of operational indicators to translate the  
702 Sendai Framework into action, Report, JRC95505, EUR 27192 EN, 2015.

703 Coughlan de Perez, E. van Aalst, M. K. et al., Action-based flood forecasting for triggering  
704 humanitarian action, *Hydrol. Earth Syst. Sci.* 20, 3549-3560, 2016. doi:10.5194/hess-20-3549-  
705 2016

706 De Bruijn, K. M., Diermanse, F. L. M., Beckers, J. V. L., An advanced method for flood risk  
707 analysis in river deltas, applied to societal flood fatality risk in the Netherlands .*Nat. Hazards*  
708 *Earth Syst. Sci.*, 14, 2767–2781, 2014, doi:10.5194/nhess-14-2767-2014.



709 Dottori F., Salamon P., Kalas M., Bianchi A., Thielen J., Feyen L., 2015. A near real-time  
710 procedure for flood hazard mapping and risk assessment in Europe. 36th IAHR World Congress  
711 28 June – 3 July, The Hague, the Netherlands.

712 EC, 2016. List of EU Solidarity Fund Interventions since 2002,  
713 [http://ec.europa.eu/regional\\_policy/sources/thefunds/doc/interventions\\_since\\_2002.pdf](http://ec.europa.eu/regional_policy/sources/thefunds/doc/interventions_since_2002.pdf)(accesse  
714 d 15-9-2016).

715 EC, 2007. Directive 2007/60/EC of the European Parliament and of the Council on the  
716 assessment and management of flood risks. Official Journal of the European Communities,  
717 Brussels,<http://eur-lex.europa.eu/legal-content/EN/TXT/?uri=CELEX%3A32007L0060>  
718 (accessed 21-10-2016).

719 ECMWF, 2014. EFAS Bulletin April – May 2014, [https://www.efas.eu/efas-bulletins/1801-](https://www.efas.eu/efas-bulletins/1801-efas-bulletin-april-may-2014-issue-20143.html)  
720 [efas-bulletin-april-may-2014-issue-20143.html](https://www.efas.eu/efas-bulletins/1801-efas-bulletin-april-may-2014-issue-20143.html) (accessed 21-10-2015).

721 Emerton, R., Stephens, E.M., Pappenberger, F., Pagano, T.C., Weerts, A.H., Wood, A.W.,  
722 Salamon, P., Brown, J.D., Hjerdt, N., Donnelly, C., Baugh, C.A., Cloke, H.L., 2016. Continental  
723 and global scale flood forecasting systems. *WIREs Water* 3, 391–418, doi:10.1002/wat2.1137.

724 ESRI map of World Cities,  
725 <https://www.arcgis.com/home/item.html?id=dfab3b294ab24961899b2a98e9e8cd3d> (accessed 6-  
726 3-2017).

727 Geoportal GeoSerbia, <http://www.geosrbija.rs/> (accessed 21-10-2016).

728 Huizinga H. J. (2007). Flood damage functions for EU member states, HKV Consultants,  
729 Implemented in the framework of the contract #382442-F1SC awarded by the European  
730 Commission – Joint Research Centre.

731 Huizinga, J., de Moel, H., Szewczyk, W. (2017). Global flood damage functions.  
732 Methodology and the database with guidelines. EUR 28552 EN. doi: 10.2760/16510

733 Jongman B., Kreibich H., Apel H., Barredo J.I., Bates P.D., Feyen L., Gericke A., Neal J.,  
734 Aerts J.C.J.H and Ward P.J (2012). Comparative flood damage model assessment: towards a  
735 European approach. *Natural Hazards and Earth System Sciences*. 12, 3733–3752.

736 Jongman, B., Hochrainer-Stigler, S., Feyen, L., Aerts, J.C.J.H., Mechler, R., Botzen, W.J.W.,  
737 Bouwer, L.M., Pflug, G., Rojas, R., Ward, P.J., 2014. Increasing stress on disaster-risk finance  
738 due to large floods. *Nat. Clim. Change* 4, 264–268. doi:<http://dx.doi.org/10.1038/nclimate2124>.

739 ICPDR – International Commission for the Protection of the Danube River and ISRBC –  
740 International Sava River Basin Commission 2015. Floods in May 2014 in the Sava River Basin.  
741 [https://www.icpdr.org/main/sites/default/files/nodes/documents/sava\\_floods\\_report.pdf](https://www.icpdr.org/main/sites/default/files/nodes/documents/sava_floods_report.pdf)  
742 (accessed 11-10-2015).

743 International Labour Group (ILO), 2014. Bosnia and Herzegovina Floods 2014: Recovery  
744 Needs Assessment. [http://www.ilo.org/global/topics/employment-promotion/recovery-and-](http://www.ilo.org/global/topics/employment-promotion/recovery-and-reconstruction/WCMS_397687/lang--en/index.htm)  
745 [reconstruction/WCMS\\_397687/lang--en/index.htm](http://www.ilo.org/global/topics/employment-promotion/recovery-and-reconstruction/WCMS_397687/lang--en/index.htm) (accessed 6-4-2017).

746 IRDR – Integrated Research on Disaster Risk: Guidelines on Measuring Losses from  
747 Disasters: Human and Economic Impact Indicators, Integrated Research on Disaster Risk,  
748 Beijing, IRDR DATA Publication No. 2, 2015.

749 Marín Herrera, M., Batista e Silva, F., Bianchi, A., Barranco, R. and Lavalle, C., 2015. A  
750 geographical database of infrastructures in Europe. JRC Technical Report, JRC99274.

751 Molinari D., Ballio F., Menoni S., 2013. Modelling the benefits of flood emergency  
752 management measures in reducing damages: A case study on Sondrio, Italy. *Nat. Hazards Earth*  
753 *Syst. Sci.*, 13, 1913–1927.

754 Molinari D., Ballio F., Handmer J., Menoni S., 2014. On the modelling of significance for  
755 flood damage assessment. *International Journal of Disaster Risk Reduction* 10, 381–391.

756 Pappenberger F., Thielen J., and Del Medico M. (2011). The impact of weather forecast  
757 improvements on large scale hydrology: analysing a decade of forecasts of the European Flood  
758 Alert System. *Hydrological Processes*, 25, 1091–1113. <http://dx.doi.org/10.1002/hyp.7772>.

759 Pappenberger F., Cloke, H. L., Parker, D.J., Wetterhall, F., Richardson, D.S, Thielen, J., 2015.  
760 The monetary benefit of early flood warnings in Europe. *Environmental Science &Policy* 51,  
761 278–291.

762 Rossi, L., Rudari, R., and the RASOR Team. RASOR Project: Rapid Analysis and  
763 Spatialisation of Risk, from Hazard to Risk using EO data. *Geophysical Research Abstracts* Vol.  
764 18, EGU2016-15073.

765 Saint-Martin, C., Fouchier, C., Douvinet, J., Javelle, P., Vinet, F., 2016. Contribution of an  
766 exposure indicator to better anticipate damages with the AIGA flood warning method: a case  
767 study in the South of France. *Geophysical Research Abstracts* Vol. 18, EGU2016-10305-4.

768 Sampson, C.C., Smith, A.M, Bates, P.D., Neal, J.C., Alfieri, L., Freer, J.E., 2015. A High  
769 Resolution Global Flood Hazard Model. *Water Resour. Res.* 51-9, 7358-7381, doi:  
770 10.1002/2015WR016954.

771 Schulz, A., Kiesel, J., Kling, H., Preishuber M., Petersen G., 2015. An online system for rapid  
772 and simultaneous flood mapping scenario simulations - the Zambezi Flood DSS. *Geophysical*  
773 *Research Abstracts* Vol. 17, EGU2015-6876.

774 Thielen J., Bartholmes J., Ramos M.H., and De Roo A. (2009). The European flood alert  
775 system – part 1: concept and development. *Hydrol. Earth Syst. Sci.* 13, 125–140.

776 Tanoue, M., Hirabayashi, Y., Ikeuchi, H., 2016. Global-scale river flood vulnerability in the  
777 last 50 years. *Scientific Reports*, 6, 36021.

778 UNDAC - United Nations Disaster Assessment and Coordination Team, 2014. Mission to  
779 Serbia – Floods 18-31 May 2014, end of mission report.

780 United Nations, Office for Outer Space Affairs, 2014. Floods in Bakans, [http://www.un-](http://www.un-spider.org/advisory-support/emergency-support/8497/floods-balkans)  
781 [spider.org/advisory-support/emergency-support/8497/floods-balkans](http://www.un-spider.org/advisory-support/emergency-support/8497/floods-balkans)(accessed 6-4-2017).

782 Van der Knijff, J.M., Younis, J., de Roo, A.P.J., 2010. LISFLOOD: a GIS-based  
783 distributed model for river basin scale water balance and flood simulation. *Int. J. Geogr. Inf. Sci.*  
784 24, 189–212.

785 Vogt et al., 2007. A pan-European river and catchment database, JRC Reference Reports,  
786 doi:0.2788/35907.

787       Wagenaar, D. J., de Bruijn, K. M., Bouwer, L. M., and de Moel, H.: Uncertainty in flood  
788 damage estimates and its potential effect on investment decisions, *Nat. Hazards Earth Syst. Sci.*,  
789 16, 1-14, doi:10.5194/nhess-16-1-2016, 2016.

790       Ward, P.J., Jongman, B., Salamon, P., Simpson, A., Bates, P., De Groeve, T., Muis, S., De  
791 Perez, E.C., Rudari, R., Trigg, M.A., Winsemius, H.C., 2015. Usefulness and limitations of global  
792 flood risk models. *Nat. Clim. Change*, 5 (8), 712-715.

793       Wikipedia. Poplave u istočnoj Hrvatskoj u svibnju 2014 (accessed 21-10-2016).  
794  
795